BMB
Reports

BMB Rep. 2024; 57(2): 92-97
www.bmbreports.org

Glucosamine increases macrophage lipid accumulation by regulating the mammalian target of rapamycin signaling pathway

Sang-Min Kim[1,#], *Dong Yeol Kim*[1,#], *Jiwon Park*[1], *Young-Ah Moon*[2] *& Inn-Oc Han*[1,*]

[1]Department of Biomedical Science, Program in Biomedical Science and Engineering, Inha University, Incheon 22212, [2]Department of Molecular Medicine, College of Medicine, Inha University, Incheon 22212, Korea

Elevated blood glucose is associated with an increased risk of atherosclerosis. Data from the current study showed that glucosamine (GlcN), a normal glucose metabolite of the hexosamine biosynthetic pathway (HBP), promoted lipid accumulation in RAW264.7 macrophage cells. Oleic acid- and lipopolysaccharide (LPS)-induced lipid accumulation was further enhanced by GlcN in RAW264.7 cells, although there was no a significant change in the rate of fatty acid uptake. GlcN increased *acetyl CoA carboxylase* (*ACC*), *fatty acid synthase* (*FAS*), *scavenger receptor class A*, *liver X receptor*, and *sterol regulatory element-binding protein-1c* (*SREBP-1c*) mRNA expression, and; conversely, suppressed *ATP-binding cassette transporter A1* (*ABCA-1*) and *ABCG-1* expression. Additionally, GlcN promoted *O*-GlcNAcylation of nuclear SREBP-1 but did not affect its DNA binding activity. GlcN stimulated phosphorylation of mammalian target of rapamycin (mTOR) and S6 kinase. Rapamycin, a mTOR-specific inhibitor, suppressed GlcN-induced lipid accumulation in RAW264.7 cells. The GlcN-mediated increase in *ACC* and *FAS* mRNA was suppressed, while the decrease in *ABCA-1* and *ABCG-1* by GlcN was not significantly altered by rapamycin. Together, our results highlight the importance of the mTOR signaling pathway in GlcN-induced macrophage lipid accumulation and further support a potential link between mTOR and HBP signaling in lipogenesis. [BMB Reports 2024; 57(2): 92-97]

INTRODUCTION

Intracellular lipids are stored and metabolized in hydrophobic organelles in the macrophages. Increased macrophage lipid accumulation has been identified as a key mediator in the development of atherosclerosis by contributing to the enlargement of atherosclerotic lesions and the formation of thrombosis (1). Hyperglycemia accelerates atherosclerotic lesion progression through direct effects on genes controlling lipid metabolism in macrophages (2, 3). Among the mechanisms implicated in glucose-mediated regulation of lipid accumulation, the hexosamine pathway (HBP) has attracted significant research attention as a potential contributory factor to hyperglycemia-induced atherosclerosis (4). Hyperglycemia enhances HBP flux and induces an increase in endogenous glucosamine (GlcN), a common metabolite of HBP. Exogenous GlcN is transported into cells by glucose transporters and merges into HBP to elevate levels of UDP-N-acetyl-GlcN (UDP-GlcNAc), a substrate for transfer of *O*-GlcNAc to nuclear and cytosolic proteins by *O*-GlcNAc transferase (OGT). Altered *O*-GlcNAc signaling plays an important role in its complications including nonalcoholic fatty liver disease (NAFLD), and diabetic nephropathy and/or retinopathy (5).

The mammalian target of rapamycin (mTOR), a serine/threonine protein kinase, is an important regulator of cellular homeostasis and metabolism (6). mTOR activates and promotes protein synthesis, lipogenesis, and energy metabolism in response to high nutrient and energy conditions (6) and regulates protein synthesis through direct phosphorylation of the downstream target p70S6K. Previous studies indicate that mTOR enhances foam cell formation and its inhibition suppresses atherosclerosis in ApoE$^{-/-}$ mice (7). Furthermore, evidence showing that rapamycin, a mTOR-specific inhibitor, reduces lipid accumulation in cells and prevents plaque formation, is documented in the literature (8, 9).

In the present study, we examined the effect and regulatory mechanism of macrophage lipid accumulation in response to increased HBP flux by GlcN. We demonstrated that GlcN enhances intracellular lipid accumulation, potentially by regulating lipogenesis in macrophages. We suggested that increased HBP flux regulates mTOR-dependent lipogenesis. These collective findings support the utility of enzymes in the HBP pathway as regulatory targets for therapeutic intervention in atherosclerosis.

*Corresponding author. Tel: +82-32-860-9854; Fax: +82-32-860-9851; E-mail: iohan@inha.ac.kr
#These authors contributed equally to this work.

https://doi.org/10.5483/BMBRep.2023-0158

Received 31 August 2023, Revised 5 October 2023, Accepted 3 November 2023, Published online 4 January 2024

Keywords: Atherosclerosis, Foam cell, Hexosamine, mTOR

ISSN: 1976-670X (electronic edition)

RESULTS

GlcN promotes lipid accumulation in RAW264.7 cells

RAW264.7 murine macrophage cells were incubated with various concentrations of glucose for 24 and intracellular lipid accumulation was examined by staining with Oil Red O (ORO). Glucose treatment for 24 h did not lead to a significant increase in the cellular lipid content (Fig. 1A). GlcN (3, 4, and 5 mM) induced an increase in cellular lipid levels at 24 h (Fig. 1B). Electron microscopy examination of GlcN-treated RAW264.7 cells revealed larger and emptier vacuoles compared to the controls, presumably due to increased lipid droplet deposits in the cytoplasm (Fig. 1C).

Oleic acid (OA) treatment of RAW264.7 cells induced an increase in the lipid content, which was further enhanced by GlcN co-treatment (Fig. 1D). In contrast, co-treatment with GalN and ManN did not affect OA-induced lipid accumulation. Lipopolysaccharide (LPS) has been shown to enhance lipid accumulation in macrophages by increasing glucose and lipid uptake (10). In our experiments, while both LPS and GlcN individually increased macrophage lipid accumulation, GlcN did not potentiate the LPS-induced increase in lipid accumulation. However, both LPS and GlcN showed potentiation effects on OA-induced lipid accumulation (Fig. 1E). Next, we assessed the effects of GlcN and/or LPS on the uptake of fatty acids (FA). Interestingly, while LPS treatment increased FA uptake as described previously (10), GlcN did not promote FA uptake in the presence or absence of LPS (Fig. 1F).

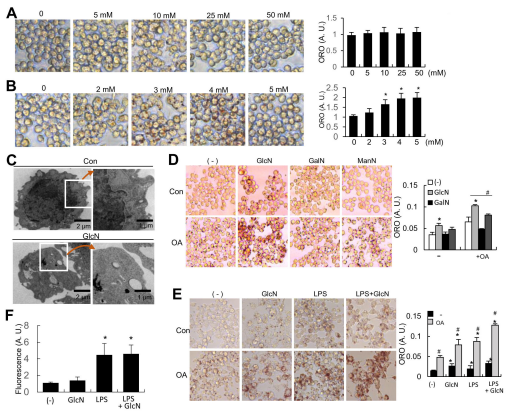

Fig. 1. Effects of GlcN, OA, LPS and amine sugars on lipid accumulation in RAW264.7 cells. (A, B) RAW264.7 cells were treated with the indicated concentrations of glucose (A) or GlcN (B) for 24 hrs. ORO staining was performed at 24 hrs, extracted using isopropanol, and quantified via spectrophotometry at 520 nm. (C) RAW264.7 cells were treated with 3 mM GlcN for 24 hrs. Representative transmission electron microscopy (TEM) images showing lipid droplets in cells. (D) RAW264.7 cells were pre-treated with 3 mM GlcN, GalN, or ManN for 1 hr, followed by treatment with 100 μM OA for 24 hrs. ORO staining was performed and quantified. (E) RAW264.7 cells were pre-treated with GlcN for 1 hr and treated with OA and/or 0.1 μg /mL LPS for 24 hrs, followed by quantification of ORO staining. Data are representative of three independent experiments and graphs present the arbitrary unit of quantification normalized to protein content. (F) RAW264.7 cells were treated with GlcN (3 mM) and/or LPS (0.1 μg/ml) for 12 hrs, subsequently incubated with BODIPY^{TM} FL C16 for 3 min, and fluorescence/well read. *P < 0.05 versus control; $^{\#}$P < 0.05 versus OA-untreated group.

GlcN induces lipid accumulation in an ER stress-independent manner and enhances mRNA expression of lipogenic genes in RAW264.7 cells

To investigate the role of ER stress in lipid accumulation induced by GlcN and LPS, we assessed the effects of the ER stress inhibitor, 4-phenylbutyric acid (PBA), on lipid accumulation. Treatment with PBA did not significantly alter the lipid levels induced by GlcN and LPS in the cells (Supplementary Fig. A). Both GlcN and LPS promoted mRNA and protein levels of the ER stress regulatory proteins, CHOP and GRP78, which were inhibited under conditions of treatment with PBA (Supplementary Fig. B, C).

Next, we examined the expressions of key lipogenic genes in GlcN-treated RAW264.7 cells. GlcN treatment for 6 or 24 h induced a dose-dependent increase in mRNA expression of *acetyl-CoA carboxylase* (*ACC*) and *fatty acid synthase* (*FAS*) (Fig. 2A). Additionally, mRNA levels of *scavenger receptor class A type 1* (*SR-A1*), *liver X receptor* (*LXR*), and *sterol regulatory*

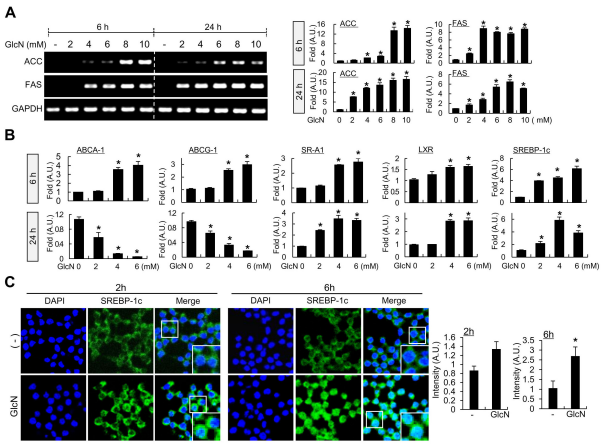

Fig. 2. Regulation of lipogenesis factors in response to GlcN. (A) RAW264.7 cells were treated with GlcN (3 mM) for 6 or 24 hrs. mRNA levels were assessed via RT-PCR (left panel) and quantitative real-time PCR (right panel) using GAPDH as an internal control. (B) RAW264.7 cells were treated with the indicated concentrations of GlcN for 6 or 24 hrs. mRNA levels were assessed via quantitative real-time PCR. (C) RAW264.7 cells were pre-treated with 3 mM GlcN for 2 or 6 hrs. Representative confocal images (× 40) of DAPI (blue), SREBP-1 (green), and merged immunofluorescence staining in RAW264.7 cells. Graphs represent densitometric quantification of immunofluorescence. Data are representative of at least three independent experiments and graphs represent fold changes relative to control. *P < 0.05 versus control.

element-binding protein (*SREBP-1c*), a transcription factor regulating lipid metabolism, were elevated with GlcN treatment (Fig. 2B). Notably, compared with the control cells, GlcN promoted mRNA levels of *ATP binding cassette transporter A-1* (*ABCA-1*) and *ABCG-1*, lipid transporters that mediate efflux of cholesterol from cells, at 6 h but this expression was decreased at 24 h (Fig. 2B). Furthermore, the GlcN-treated group showed increased nuclear translocation of SREBP-1 compared to control at 6 h (Fig. 2C).

GlcN increases *O*-GlcNAcylation of mature SREBP-1

GlcN activates HBP and induces *O*-GlcNAcylation of nucleocytoplasmic proteins. A WGA pulldown experiment demonstrated that GlcN increases *O*-GlcNAcylation of nucleocytoplasmic proteins and the 65 kDa, mature form of SREBP-1 but not the 122 kDa precursor SREBP-1 (Fig. 3A). However, despite the increase in *O*-GlcNAcylation caused by GlcN, the DNA binding of 65 kDa SREBP-1 to the consensus SRE site was not significantly enhanced by GlcN (Fig. 3B).

GlcN increases mTOR signaling and rapamycin suppresses GlcN-induced lipid accumulation

To clarify the signaling pathways involved in GlcN-induced lipid accumulation, we examined phosphorylation of the key signaling molecule involved in lipid metabolism, mTOR. GlcN, but not LPS, stimulated phosphorylation of mTOR (Fig. 4A). Our results also showed a significant increase in phosphorylation of S6K by GlcN (Fig. 4B). Next, we examined whether rapamycin, a mTOR inhibitor, affects GlcN-induced lipid accumulation. Rapamycin suppressed GlcN-induced lipid accumulation (Fig. 4C) and phosphorylation of mTOR by GlcN (Fig. 4D, F). Additionally, rapamycin induced a decrease in mRNA expression of ACC and FAS promoted by GlcN, but did not affect the transcription of ABCA1 and ABCG1 (Fig. 4F).

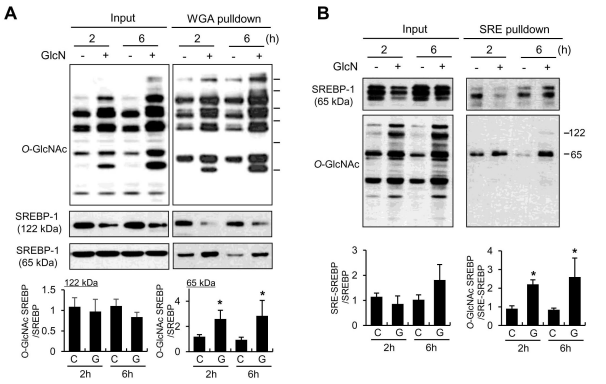

Fig. 3. GlcN-induced regulation of SREBP-1 *O*-GlcNAcylation in RAW264.7 cells. (A) RAW264.7 cells were treated with GlcN (3 mM) for 2 or 6 hrs. Total lysates and WGA-binding proteins were analyzed via western blot using RL2 and SREBP-1 antibodies. Graphs represent relative densitometric intensities of WGA-bound SREB-1 (122 and 65 kDa) normalized to input SREBP-1. (B) RAW264.7 cells were treated with the GlcN for 2 or 6 hrs. Nuclear lysates were prepared and SRE-binding proteins analyzed via western blot using RL2 and SREBP-1 antibodies. Data are representative of at least three independent experiments and graphs represent fold changes relative to control. *P $<$ 0.05 versus control.

DISCUSSION

The major finding of the present study is that GlcN, an intermediate metabolite of the HBP, promotes lipid accumulation in macrophage cells. This effect was specific to GlcN, as even

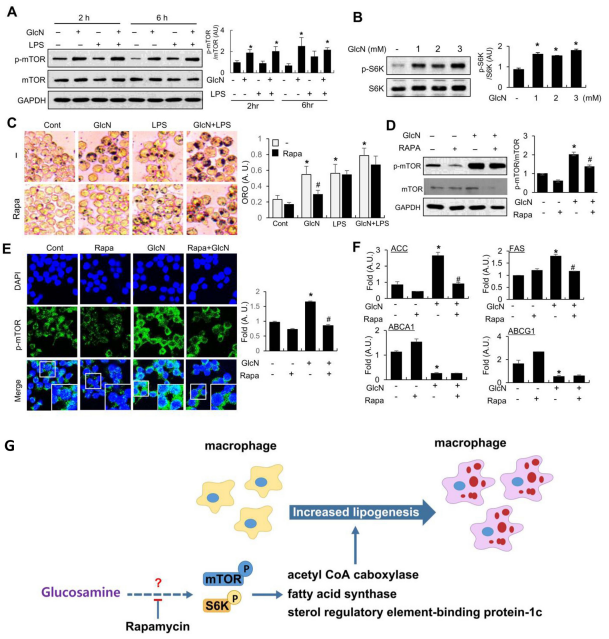

Fig. 4. Effects of rapamycin on GlcN-induced lipid accumulation in RAW264.7 cells. (A, B) (A) RAW264.7 cells were pre-treated with GlcN for 1 h, followed by treatment with LPS for 2 or 6 hrs. (B) RAW264.7 cells were treated with the GlcN for 6 hrs. Total cell lysates were prepared and western blot analysis performed using specific antibodies. (C) RAW264.7 cells were pre-treated with rapamycin (50 nM) for 30 min, followed by treatment with 3 mM GlcN for 24 or 48 hrs. ORO staining was performed at 24 hrs, extracted, and quantified. (D, E) RAW264.7 cells were pre-treated with 50 nM rapamycin for 30 min, followed by treatment with 3 mM GlcN for 6 hrs. (D) Total cell lysates were prepared and western blot analysis performed using indicated antibodies. (E) Representative confocal images (× 40) of DAPI (blue), p-mTOR (green), and merged immunofluorescence staining in RAW264.7 cells were shown. Graphs represent densitometric quantification of immunofluorescence. (F) RAW264.7 cells were treated with 3 mM GlcN for 6 hrs. *ACC*, *FAS*, *ABCA-1*, and *ABCG-1* mRNA levels were assessed via quantitative real-time PCR. Representative Western blots are shown. All densitometric quantification was conducted using Image J (NIH) and relative values presented as an arbitrary unit relative to control. (G) Summary Overview. Glucosamine enhances lipogenesis in RAW264.7 macrophage cells by activating the mTOR pathway. *P $<$ 0.05 versus control; $^{\#}$P $<$ 0.05 versus GlcN.

at very high concentrations of exogenous glucose (up to 50 mM), there was no increase in lipid synthesis. This demonstrates that GlcN can specifically enhance lipid synthesis independent of the glucose metabolic pathway. GlcN has been identified as a potent inducer of ER stress (11) and data from both animal models and cell culture experiments indicate that GlcN disrupts lipid metabolism and accelerates atherosclerosis through increased ER stress-associated macrophage apoptosis (12). However, GlcN-induced lipogenesis and lipid drop formation, which are independent of ER stress, have not attracted significant research interest to date. Our data showed that while both GlcN and LPS induced ER stress, lipid accumulation induced by both GlcN and LPS was not influenced by the ER stress inhibitor, PBA. The discrepancy between previous and current findings may stem from the GlcN dose. While previous experiments used a high concentration (15 mM) of GlcN to demonstrate ER stress involvement in lipid accumulation and apoptosis in macrophages, in our investigation lower concentrations of GlcN (1-5 mM) were used. One possible explanation is that at a lower dose, GlcN may induce lipid accumulation in an ER stress- or apoptosis-independent manner.

We have proposed several potential pathways that may contribute to GlcN-mediated macrophage lipid accumulation. One suggested mechanism is an increase in cellular glucose uptake by GlcN. Increased exogenous glucose did not further enhance lipid accumulation, indicating that GlcN is less likely to regulate the lipid content by increasing glucose uptake. Another proposal is that GlcN induces uncontrolled uptake of lipid and/or cholesterol or impairs lipid and/or cholesterol release, resulting in the accumulation of cytoplasmic lipid droplets. CD36 and SR-A are principally responsible for the binding and uptake of ox-LDL in macrophages (13), while ABCA1 and ABCG1 regulate cholesterol efflux. Our results showed upregulation of *SR-A1* and; conversely, downregulation of *ABCA1* and *ABCG1* at 24 h by GlcN, indicating the potential contribution of lipid/cholesterol uptake and efflux mechanisms to GlcN-induced macrophage lipid accumulation. Our results showed that GlcN did not increase FA uptake on its own. Third, GlcN may increase lipid synthesis by regulating the expressions or activities of lipogenic genes. In our experiments, GlcN increased the mRNA expression levels of enzymes involved in lipid synthesis, such as *FAS*, *ACC*, and *LXR*, as well as *SREBP-1*, a transcription factor responsible for regulating these enzymes. Together, our findings suggest that GlcN-induced lipid accumulation is, at least partially, attributed to the stimulation of the lipogenic process. To our knowledge, the current study is one of a few reports to document the regulation of lipogenic genes by intermediates of glucose metabolism in macrophages.

SREBP-1 is a key transcription factor for lipid metabolism in response to active glucose flux that undergoes *O*-GlcNAc modification to regulate binding to target gene (*L-PK*, *ACC*, *FAS*, and *SCD1*) promoters (14, 15). In this study, GlcN increased *O*-GlcNAcylation and nuclear localization of SREBP-1. Intriguingly; however, the DNA binding activity of SREBP-1 to its consensus binding site was not affected by GlcN, indicating that *O*-GlcNAcylation of SREBP-1 does not directly regulate its transcriptional activity. Although not confirmed in our study, there is a possibility that *O*-GlcNAcylation of SREBP could promote its cleavage, thus activating its activity.

Both mTOR and HBP pathways participate in nutrient sensing and share responses to fluctuations in nutrition, offering an interesting avenue for exploring possible interactions (16, 17). Earlier reports have shown that mTOR signaling regulates protein *O*-GlcNAcylation in hepatic and breast cancer cells (17). Moreover, mTOR signaling is activated in *O*-GlcNAcylated nucleocytoplasmic proteins, and treatment with rapamycin, a mTOR inhibitor, decreases both *O*-GlcNAcylation and mTOR phosphorylation in colon cancer cells (16), indicative of crosstalk between *O*-GlcNAcylation and mTOR signaling. It has been demonstrated that mTOR can be regulated through *O*-GlcNAcylation in hepatoma cells (18). Therefore, GlcN-induced *O*-GlcNAcylation of mTOR might regulate its phosphorylation or activity. However, the direct effects of GlcN on mTOR *O*-GlcNAcylation could not be determined through Western blotting for *O*-GlcNAcylation of mTOR or co-immunoprecipitation of OGT with mTOR in RAW264.7 cells cultured with or without GlcN. Since RL2 and CTD110.1 have limited epitope recognition for detecting *O*-GlcNAc sites in proteins, it may be necessary to employ mass spectrometry analysis to determine changes in *O*-GlcNAcylation of mTOR.

In summary, GlcN promotes lipogenesis potentially by stimulating the mTOR signaling pathway in macrophage cells (Fig. 4G). Our findings suggest that high glucose conditions supply the substrate for not only lipid synthesis but also lipogenesis via the HBP and mTOR pathways to induce lipid accumulation in macrophages. The results of the current study provide further insights into the importance of the HBP pathway in regulating lipogenesis, offering a novel paradigm to delineate the mechanisms by which increased glucose flux regulates foam cell formation.

MATERALS AND METHODS

Reagents

Reagents were purchased from Sigma Chemical (St. Louis, MO, USA) or Amresco (Cochran Road, OH, USA), unless otherwise specified.

Cell cultures

RAW264.7 murine macrophage cells (purchased from the Korean Cell Line Bank) were maintained at 37°C and 5% CO_2 in Dulbecco's Modified Eagle Medium (DMEM) supplemented with 5% fetal bovine serum (FBS; Hyclone, Utah, USA), 1 mM sodium pyruvate, 1% streptomycin and penicillin.

Oil Red O (ORO) staining

Cells were fixed in 3.5% formaldehyde for 2 min and rinsed twice with 60% isopropanol. After staining with 0.3% ORO

working solution at room temperature (RT) for 15 min, cells were washed with PBS. Stained cells were observed under a light microscope (DMIL, Leica, Wetzlar, Germany) and images obtained using TCapture software (TUCSEN). For quantitative analysis of cellular lipids, 250 μl isopropanol was added to each well of the stained culture plates. The dissolved dye was analyzed spectrophotometrically at 520 nm.

Measurement of cellular free fatty acid accumulation and uptake

Fatty acid accumulation in RAW264.7 cells was measured by exposing the cells to oleic acid (OA), following the previously described method (19). RAW264.7 cells were exposed to 0.1 mM OA in the presence or absence of GlcN, galactosamine (GalN), mannosamine (ManN) or LPS for 24 hrs. Cells were subsequently washed and stained with 0.3% ORO working solution at RT for 15-30 min.

The rate of fatty acid uptake was determined using green fluorescent fatty acid, 4,4-difluoro-5,7-dimethyl-4-bora-3α,4α-diaza-s-indacene-3-hexadecanoic acid (BODIPY™ FL C_{16}, Thermo Fisher Scientific, MA, USA). Cells were treated with LPS and/or GlcN for 12 hrs, washed twice with PBS, and incubated with 1 μg/ml BODIPY™ FL C16 for 3 min at RT. After an four washes, the fluorescence/well was measured (S1LFA; Biotek, VT, USA).

Transmission electron microscopy (TEM)

RAW264.7 cells (1×10^7) were fixed for 30 min at RT in a mixture of freshly prepared 1.5% glutaraldehyde and 4% PFA in 1X PBS (pH 7.4), post-fixed in 1% phosphate-buffered osmium tetroxide, dehydrated using a graded ethanol series, and embedded in Epon 812. After incubation for 48 hrs at 60°C, ultrathin sections (60 nm) were cut and mounted on grids. Samples were examined using a LEO 912 OMEGA transmission electron microscope (JEM-2100F, Zeiss) at 120 kV accelerating voltage. Digital images were obtained using a side-mounted MegaView III TEM CCD camera.

Reverse transcription PCR

Total RNA was extracted with TRIzol™ (Invitrogen, Carlsbad, CA, USA). Complementary DNA was synthesized from 2 μg of RNA with GoScript™ Reverse Transcriptase (Promega, Madison, WI, USA) according to the manufacturer's protocol. PCR was performed using mouse specific primers (GRP78, F: GGTGCA GCAGGACATCAAGTT, R: CCCACCTCCAATATCAACTTGA; CHOP, F: CTGCCTTTCACCTTGGAGAC, R: CGTTTCCTGGG GATGAGATA, ACC, F: TGCAGCACAGCTCCAGATTG, R: AG CAGTGCCCGAACTGAGAA, FAS, F: CTGGACTCGCTCATGG GTGT, R: GTGGAACACGGTGGTGGAAC, ABCA-1, F: AGTG ATAATCAAAGTCAAAGGCACAC, R: AGCAACTTGGCACTAG TAACTCTG, ABCG-1, F: CAACCCGCCTGTCATGTTCT, R: AT CCCCCGTACTCCCCTGATG, SR-A1, F: GGCTCTGCCCTCATG AACAA, R: TGGTCAGTTGCCATGCTGAA, LXR, F: CCCCATG GACACCTACATGC, R: GACACGATGGCCAGCTCAGT, SREBP-1c, F: TAGTGTTGGCCTGCTTGGCT, R: CAGGCCAGATCCA GGTTTGA, GAPDH, F: TCATTGACCTCAACTACAGGT, R: C TAAGCAGTTGGTGGTGCAG). For quantitative real-time PCR experiments, cDNAs were amplified with SYBR Green Real-time PCR Master Mix (Toyobo, Osaka, Japan). All results were normalized to GAPDH expression.

Western blot analysis

Total cell lysates were prepared using NP-40 lysis buffer (150 mM NaCl, 50 mM Tris-HCl pH 8.0, 0.5% NP-40 containing protease and phosphatase inhibitors). Separation of nuclear and cytosolic fractions were performed as described previously (20). Protein concentrations were determined using the Bradford assay. Total proteins (20 μg) were separated via SDS-PAGE and transferred onto nitrocellulose membranes (Amersham Biosciences, NJ, USA), which were blocked with 5% non-fat milk. Next, membranes were incubated with antibodies against anti-GRP78, anti-phospho-mTOR, anti-mTOR, anti-phospho-S6K, anti-S6K, and anti-GAPDH (Cell Signaling Technology, MA, USA). After washing with TBS-T, horseradish peroxidase (HRP)-conjugated secondary antibodies (Amersham Biosciences; 1: 10,000 dilution) were applied and images developed with the Enhanced Chemiluminescence (ECL) detection system (Amersham Biosciences). Densitometric quantification of protein bands was performed using Image J (NIH).

Streptavidin-agarose pull down assay

Biotin pull-down assays were performed as described previously (20). A 24 nucleotide sequence containing the SRE binding site (−75 to −52, 5′ GCTGTCAGCCCATGTGGCGT GGCC) of the fatty acid synthase promoter. Only the upper strand is shown. Two biotinylated complementary DNAs were synthesized (Bioneer Corporation, Daejeon, Korea) and annealed. Binding assays were performed by incubating 500 μg nuclear proteins with 2 μg biotinylated DNA probe and 25 μl streptavidin-conjugated agarose beads for 1 hr. DNA-protein complexes were analyzed via western blot using the indicated antibodies.

Wheat germ agglutinin (WGA) pulldown assay

Cells were lysed with NP-40 lysis buffer. For the WGA pull-down assay, 1 mg cell lysate was incubated with WGA-agarose beads for 1 hr at 4°C and the precipitated proteins analyzed via western blot. Proteins (20-40 μg each) were separated via SDS-PAGE and subjected to Western blot analysis using antibodies against anti-O-GlcNAc CTD110.6 (Covance, Berkeley, CA, USA), and SREBP-1 (Novus Biologicals, Denver, CO, USA).

Immunofluorescence microscopy

Cells were fixed in 4% paraformaldehyde and permeabilized with 0.1% Triton X-100 in PBS. After blocking with 5% BSA, cells were incubated with anti-phospho-mTOR antibody (Cell Signaling Technology) overnight at 4°C, followed by FITC-conjugated secondary antibody (Molecular Probes, Eugene,

OR, USA) for 1 hr. Nuclei were counterstained with DAPI. Slides were coverslipped and viewed using confocal laser scanning microscopy (Zeiss LSM 510 META).

Statistical analysis

Data are expressed as means ± SEM. Student's *t*-test was applied to compare two samples, while for more than two samples, one-way ANOVA using Prism 6 software (GraphPad, San Diego, CA, USA) was performed. Differences were considered statistically significant at $P < 0.05$.

ACKNOWLEDGEMENTS

This work was supported by National Research Foundation (NRF) of Korea Grants (NRF-2021R1A2C1012480) and research grant of Inha University.

CONFLICTS OF INTEREST

The authors have no conflicting interests.

REFERENCES

1. McLaren JE, Michael DR, Ashlin TG and Ramji DP (2011) Cytokines, macrophage lipid metabolism and foam cells: implications for cardiovascular disease therapy. Prog Lipid Res 50, 331-347
2. Fukuhara-Takaki K, Sakai M, Sakamoto Y, Takeya M and Horiuchi S (2005) Expression of class A scavenger receptor is enhanced by high glucose in vitro and under diabetic conditions in vivo: one mechanism for an increased rate of atherosclerosis in diabetes. J Biol Chem 280, 3355-3364
3. O'Rourke L, Gronning LM, Yeaman SJ, and Shepherd PR (2002) Glucose-dependent regulation of cholesterol ester metabolism in macrophages by insulin and leptin. J Biol Chem 277, 42557-42562
4. McClain DA and Crook ED (1996) Hexosamines and insulin resistance. Diabetes 45, 1003-1009
5. Ma J and Hart GW (2013) Protein O-GlcNAcylation in diabetes and diabetic complications. Expert Rev Proteomics 10, 365-380
6. Laplante M and Sabatini DM (2012) mTOR signaling in growth control and disease. Cell 149, 274-293
7. Wang X, Li L, Niu X et al (2014) mTOR enhances foam cell formation by suppressing the autophagy pathway. DNA Cell Biol 33, 198-204
8. Cruzado JM (2008) Nonimmunosuppressive effects of mammalian target of rapamycin inhibitors. Transplant Rev (Orlando) 22, 73-81
9. Basso MD, Nambi P and Adelman SJ (2003) Effect of sirolimus on the cholesterol content of aortic arch in ApoE knockout mice. Transplant Proc 35, 3136-3138
10. Feingold KR, Shigenaga JK, Kazemi MR et al (2012) Mechanisms of triglyceride accumulation in activated macrophages. J Leukoc Biol 92, 829-839
11. Qiu W, Avramoglu RK, Rutledge AC, Tsai J and Adeli K (2006) Mechanisms of glucosamine-induced suppression of the hepatic assembly and secretion of apolipoprotein B-100-containing lipoproteins. J Lipid Res 47, 1749-1761
12. Beriault DR, Sharma S, Shi Y, Khan MI and Werstuck GH (2011) Glucosamine-supplementation promotes endoplasmic reticulum stress, hepatic steatosis and accelerated atherogenesis in apoE−/− mice. Atherosclerosis 219, 134-140
13. Chistiakov DA, Bobryshev YV and Orekhov AN (2016) Macrophage-mediated cholesterol handling in atherosclerosis. J Cell Mol Med 20, 17-28
14. Sodi VL, Bacigalupa ZA, Ferrer CM et al (2018) Nutrient sensor O-GlcNAc transferase controls cancer lipid metabolism via SREBP-1 regulation. Oncogene 37, 924-934
15. Guinez C, Filhoulaud G, Rayah-Benhamed F et al (2011) O-GlcNAcylation increases ChREBP protein content and transcriptional activity in the liver. Diabetes 60, 1399-1413
16. Very N, Steenackers A, Dubuquoy C et al (2018) Cross regulation between mTOR signaling and O-GlcNAcylation. J Bioenerg Biomembr 50, 213-222
17. Sodi VL, Khaku S, Krutilina R et al (2015) mTOR/MYC axis regulates O-GlcNAc transferase expression and O-GlcNAcylation in breast cancer. Mol Cancer Res 13, 923-933
18. Wang X, Lin Y, Liu S et al (2020) O-GlcNAcylation modulates HBV replication through regulating cellular autophagy at multiple levels. FASEB J 34, 14473-14489
19. Lennon R, Pons D, Sabin MA et al (2009) Saturated fatty acids induce insulin resistance in human podocytes: implications for diabetic nephropathy. Nephrol Dial Transplant 24, 3288-3296
20. Hwang SY, Hwang JS, Kim SY and Han IO (2013) O-GlcNAcylation and p50/p105 binding of c-Rel are dynamically regulated by LPS and glucosamine in BV2 microglia cells. Br J Pharmacol 169, 1551-1560